

ANISOTROPY IN *c*-AXIS ORIENTED $\text{YBa}_2\text{Cu}_3\text{O}_{7-\delta}$ **R.L. LICHTI, T.R. ADAMS***Physics Department, Texas Tech University, Lubbock, TX 79409, U.S.A.***D.W. COOKE, R.S. KWOK***Los Alamos National Laboratory, Los Alamos, NM 87545, U.S.A.***C. BOEKEMA, J.C. LAM***Physics Department, San Jose State University, San Jose, CA 95192, U.S.A.***D.E. FARRELL and N. BANSAL***Physics Department, Case Western Reserve University, Cleveland, OH 44106, U.S.A.*

Muon spin relaxation (μSR) data taken at LAMPF on a *c*-axis oriented fine powder sample of $\text{YBa}_2\text{Cu}_3\text{O}_{7-\delta}$ (YBCO) embedded in epoxy are analyzed for relaxation rate anisotropy. Clear differences beyond simple magnetic field penetration depth anisotropy are observed for $\mathbf{B} \parallel c$ and $\mathbf{B} \perp c$. The low-temperature anisotropy ratio is consistent with oriented ceramic data. Small crystallite size and anisotropic flux pinning characteristics are suggested as the fundamental cause of the additional effects.

1. Introduction

Anisotropy in the superconducting properties of the copper oxide high-temperature superconductors (HTSC) directly shows the planar nature of the superconductivity in these materials. Numerical values for the anisotropy ratios provide important checks on theoretical models, determine the extent of 2-D localization of the superconducting wavefunctions, and provide evidence of the importance of grain and twin boundaries or intrinsic defects in limiting the planar characteristics.

Muon spin relaxation (μSR) yielded early measurements of the bulk magnetic field penetration depths in HTSC materials [1–3]. However, its use for anisotropy determination has been limited by lack of suitable large single crystal samples. A group from TRIUMF has published [4] data for a mosaic of single crystals of $\text{YBa}_2\text{Cu}_3\text{O}_{7-\delta}$ (YBCO). Results for a *c*-axis oriented ($\pm 9^\circ$) polycrystalline YBCO sample, also from TRIUMF [5], indicate a μSR anisotropy ratio of $\sigma_{\parallel}/\sigma_{\perp} = 2.0 \pm 0.1$ over a very wide temperature range below T_c . A group at PSI report [6] a much larger anisotropy ratio but smaller rate constants, implying

considerably longer penetration depths. A group working at ISIS and PSI, also with a mosaic of single crystals, has obtained the full angular dependence (with $\sigma_{\parallel}/\sigma_{\perp} = 5.0 \pm 0.2$) [7]. None of the published μ SR data sets show much temperature dependence in the relaxation (or penetration depth) anisotropy, except just below T_c .

In this contribution we report μ SR measurements of the anisotropy ratio for YBCO, performed on a single disk-shaped sample of *c*-axis oriented powder embedded in epoxy. The data were taken at LAMPF in a transverse applied field of 500 mT. These data yield values for the low temperature relaxation rates and anisotropy ratio which are reasonably consistent with the TRIUMF results. However, we observe definite differences in the character of the μ SR data for $\mathbf{B} \parallel \mathbf{c}$ and $\mathbf{B} \perp \mathbf{c}$ in addition to penetration depth anisotropy. Because of the relatively low statistics and problems inherent in accurately removing the μ SR signal due to the embedding epoxy, a number of data fits were performed using different basic fitting methods, various time limits, and with subsets of the fit parameters fixed. Here we discuss several important results from these fits, and general conclusions regarding possible origins of the observed differences for parallel and perpendicular fields.

2. Sample characterization

The oriented YBCO sample used in this work was prepared at Case Western Reserve using the magnetic alignment technique developed there [8]. Samples with the best *c*-axis alignment were selected for the μ SR measurements. Very narrow X-ray rocking curves were a primary selection criteria, and FWHM widths of less than 1° show the excellent *c*-axis alignment of the crystallites. The volume packing ratio is about 20% YBCO, implying reasonable isolation of individual grains (average size $\sim 25 \mu\text{m}$). The *c*-axis orientation lies in the plane of the epoxy disk for the sample on which all of the μ SR data reported here were taken. Rotation of the disk about the muon beam (initial muon polarization) direction provided the appropriate *c*-axis orientation relative to the transverse applied field. Superconducting properties of this sample were determined using magnetic susceptibility and ac inductive techniques, which gave $T_c = 92 \text{ K}$ and a transition width of less than 1 K.

3. Data and results

All the data reported here were taken in a 500 mT field applied transverse to the initial muon polarization direction. Relaxation measurements were performed for successively higher temperatures following initial cooling to $\sim 5 \text{ K}$. The epoxy yielded a μ SR signal which was roughly a third of the total intensity and

had a temperature independent asymmetry and linewidth. This signal was initially fit along with that from YBCO and the parameters agreed with those from an epoxy blank. For the final analysis, the parameters for the epoxy signal were fixed at average values from the full set of data, and only the YBCO signal parameters were varied. The epoxy rate constant of $0.20 \pm 0.01 \mu\text{s}^{-1}$ is almost identical to that for ceramic YBCO above T_c , thus data above 100 K will not be discussed further.

Although the *c*-axis alignment within the sample disk was $\pm 1^\circ$ or better, the actual accuracy of the **B** to *c* orientation due to the physical alignment of the sample disk was estimated to be $\pm 2-3^\circ$. The orientational accuracy for **B** \perp *c* was roughly the same, however data characteristics make that alignment much less critical.

The μSR data from this sample show clear differences between **B** \parallel *c* and **B** \perp *c*. The easiest to quantify is in the temperature dependence of the Gaussian relaxation rates. When a single YBCO signal is assumed, the rate constant for **B** \parallel *c* continues to increase significantly with decreasing temperature, while for **B** \perp *c* the rate is nearly constant for the lowest temperatures. Fit results displayed in fig. 1 illustrate this trend, along with the temperature dependent relaxation anisotropy ($\sigma_{\parallel}/\sigma_{\perp}$) which results. This particular fit allowed the phases for the four positron decay directions to vary independently, a procedure which resulted in the smallest errors and least scatter for the rate constants, but produced larger than the statistically expected variations in frequencies and phases. Several other procedures, such as fixing the phases at standard or average values, gave smoother frequency curves but significantly increased the rate constant errors and scatter. All of these initial fits indicated a difference in the relaxation temperature dependence for the two field directions and an increase in anisotropy at low temperatures.

Several additional qualitative differences between the \parallel and \perp data were observed. 1) The relaxation rate for **B** \parallel *c* increased when the time limits on the fitted data were shortened to $< 2 \mu\text{s}$, while no time-limit dependence was found for **B** \perp *c*. 2) There were much larger phase variations in the **B** \parallel *c* data fits than for **B** \perp *c*. 3) Careful examination of the statistics showed considerably larger differences in frequencies and phases for the upper and lower positron directions compared to the forward and backward directions, again more important for the **B** \parallel *c* case.

Several of these observations appear to be qualitatively consistent with a possible rotation of the field inside a superconducting grain away from the applied field direction. Such an effect should be expected due to penetration depth anisotropy [9] and differences in flux pinning characteristics [10] for applied field directions parallel and normal to the superconducting planes. Field rotation would occur most strongly for **B** near the *c*-axis, and should be non-existent for **B** \perp *c*. Perfect alignment of **B** \parallel *c* should also eliminate such effects.

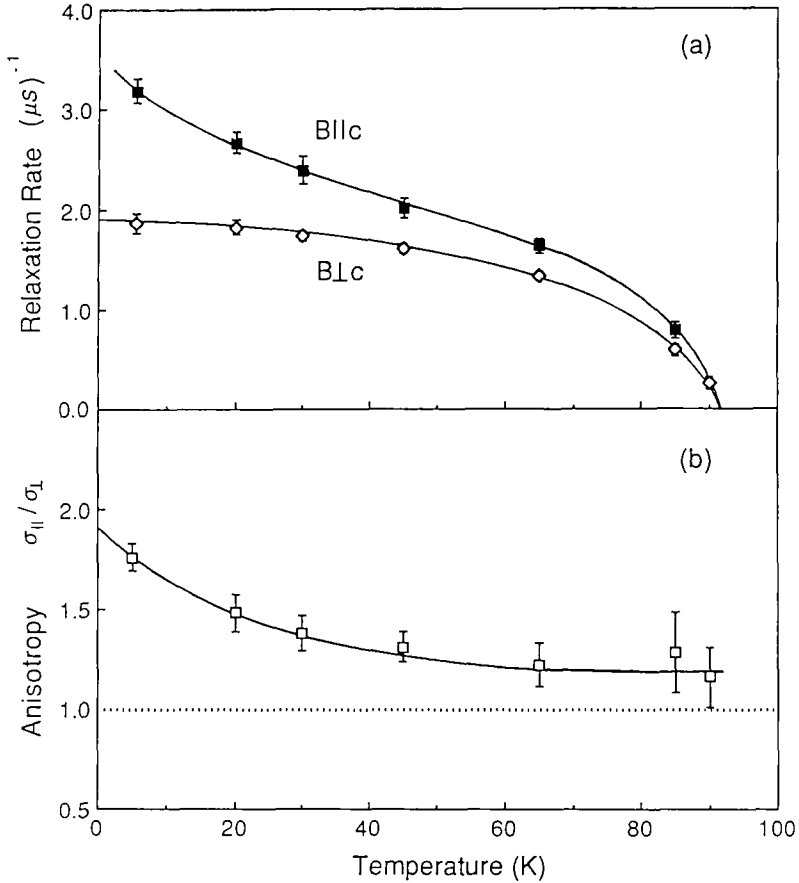


Fig. 1. Temperature dependence of a) the Gaussian μSR rates for $B \parallel c$ and $B \perp c$ in superconducting *c*-axis oriented YBCO from a single-signal analysis, and b) the resulting relaxation anisotropy ratio.

The short-time-limit rate dependence strongly implies that an additional signal is present in the $B \parallel c$ data. Therefore, we attempted a fit with two YBCO signals. Fig. 2 shows the resulting relaxation rates from a three signal fit with all YBCO parameters free, while only the phase was allowed to vary for the epoxy signal. The signal with the larger rate constant typically accounted for 70–80% of the YBCO intensity. Phases were quite close to standard values in this fit, lending additional credibility to the two-YBCO-signal assumption. Because of the large errors very little can be concluded about the weaker signal, except to note that the rate constants are more or less consistent with those published by the PSI group [6], while the larger rates are consistent with those from the TRIUMF data [4,5]. Frequency shifts imply that both of these signals arise from superconducting regions. No clear temperature dependence could be discerned in the relative intensities.

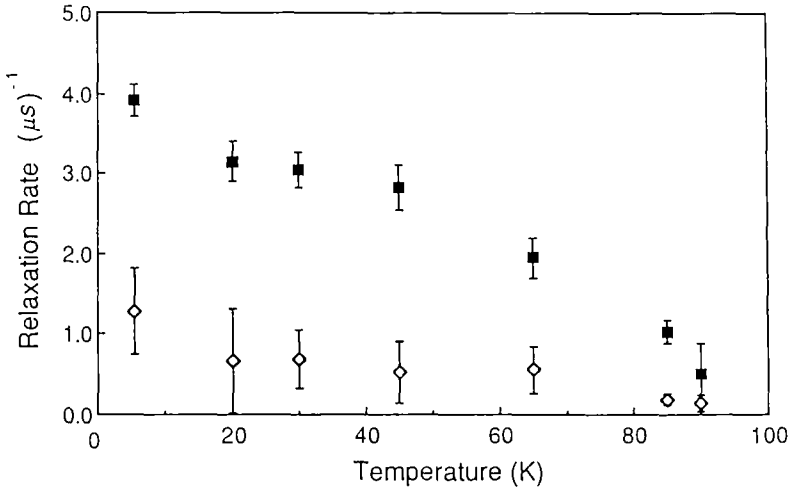


Fig. 2. Temperature dependence of Gaussian relaxation rates for $\mathbf{B} \parallel \mathbf{c}$ assuming two μSR signals for superconducting *c*-axis oriented YBCO.

A similar search for an additional signal was carried out for the $\mathbf{B} \perp \mathbf{c}$ data, however, no detectable additional signal was found. This is consistent with the qualitative differences observed in the single-signal fits. Since these data sets were taken one after the other on the same sample, this result is important and may provide a clue as to the origin of the two superconducting μSR signals sometimes seen in presumably homogeneous ceramic HTSC samples.

In order to discuss the relaxation anisotropy for the two signal fits, the more dominant of the two signals for $\mathbf{B} \parallel \mathbf{c}$ was compared to the single-signal results for $\mathbf{B} \perp \mathbf{c}$. While the errors are larger, the two-signal anisotropy ratio is much less temperature dependent than that shown in fig. 1b, and is reasonably consistent with the ratio extracted from published TRIUMF oriented polycrystal data [5]. At 5 K our data yield an anisotropy ratio of 2.1 ± 0.2 for the dominant parallel signal, and averaged over the full $T < 90$ K temperature range the ratio is 1.77 ± 0.12 .

Two other observations are relevant. First, the temperature dependence for the penetration depth as extracted from the $\mathbf{B} \perp \mathbf{c}$ data is consistent with the clean local limit for strong coupling when compared to various theoretical curves in an analysis similar to ones we have published for other samples [11]. For $\mathbf{B} \parallel \mathbf{c}$, neither the dominant of two signals, nor the single-signal result follows any standard curve. Second, at 5 K the relaxation rate for \mathbf{B} at 60° to \mathbf{c} , the single point taken at an intermediate angle, is within errors of the $\mathbf{B} \perp \mathbf{c}$ value.

4. Discussion and conclusion

The μ SR data and fits discussed above indicate clear differences beyond simple anisotropy in the relaxation rates for $\mathbf{B} \parallel c$ and $\mathbf{B} \perp c$, and thus in the penetration depths or internal field distributions, for small-grain *c*-axis oriented YBCO powder. The presence of two signals from superconducting grains for $\mathbf{B} \parallel c$ while only one is seen for $\mathbf{B} \perp c$, and the standard temperature dependence observed for $\mathbf{B} \perp c$, suggest that the cause of these differences must lie with the response of small isolated superconducting grains to a *c*-axis directed applied field.

A possible explanation of these effects is that a nearly parallel applied field is either strongly pinned in any particular crystallite, or else the internal field is free to rotate away from the *c*-axis and may do so if there is a significant perpendicular component. In this scenario the signal with the larger intensity and higher relaxation rate would be from those grains where the field is pinned, and the weaker signal from those for which the field has rotated away from the *c*-axis. An alternative picture leading to similar results is that small size and details of crystallite shape and surface conditions could allow the flux lines to locally distort in order to penetrate a small percentage of grains via the easy flux flow within superconducting planes rather than in the normal direction. Both of these suggestions are tentative, based more on feasibility and consistency arguments than on any hard evidence. Clearly, more detailed experiments and a quantitative model is required before a firm conclusion can be drawn.

One final comment is in order. A rough estimate of the time or temperature parameters related to such an effect can be made from the single-signal temperature-dependent anisotropy ratio from fig. 1b. Without some independent measure of the time/temperature scale for the field-rotation phenomena, it is not clear whether time or temperature is the limiting parameter in our data. If temperature is the relevant variable, then the decay of the low temperature anisotropy ratio leads to a pinning strength roughly equivalent to 24 K for fields in the *c*-direction. If time is the important variable, then the field-rotation time constant is quite long, approximately 5–7 hr. The pinning strength–temperature picture would seem to be the more feasible interpretation.

In conclusion, we have investigated the μ SR anisotropy in a *c*-axis oriented fine powder sample of YBCO and observe clear differences between the $\mathbf{B} \parallel c$ and $\mathbf{B} \perp c$ data beyond simple penetration depth anisotropy. Comparison with μ SR data for single-crystal and oriented ceramic samples implies that the observed differences primarily arise for $\mathbf{B} \parallel c$. Small particle size and anisotropic flux pinning characteristics may provide the underlying cause of the observed effects.

Acknowledgements

Portions of this work were supported by the Robert A. Welch Foundation, the Research Corporation, and the San Jose State University Foundation.

References

- [1] G. Aepli et al., *Phys. Rev. B* 35 (1987) 7129;
W.J. Kossler et al., *Phys. Rev. B* 35 (1987) 7133;
R. Wäppling et al., *Phys. Lett.* 122A (1987) 209;
F.N. Gyax et al., *Europhys. Lett.* 4 (1987) 473.
- [2] D.R. Harshman et al., *Phys. Rev. B* 36 (1987) 2386;
D.W. Cooke, et al., *Phys. Rev. B* 37 (1988) 9401.
- [3] Y.J. Uemura et al., *Phys. Rev. B* 38 (1988) 909.
- [4] D.R. Harshman et al., *Phys. Rev. B* 39 (1989) 851.
- [5] Y.J. Uemura et al., *J. de Phys. Colloq.* 49 (1988) 2087.
- [6] B. Pümpin et al., *Physica C* 162–164 (1989) 151.
- [7] E.M. Forgan et al., *Superconductor Science and Technology* 3 (1990) 217 and *Prog. High Temp. Superconductivity* 21 (1990) 215.
- [8] D.E. Farrell et al., *Phys. Rev. B* 36 (1987) 4025.
- [9] L.J. Campbell, M.M. Doria, and V.G. Kogan, *Phys. Rev. B* 38 (1988) 2439.
- [10] L. Fruchter et al., *J. de Phys. Colloq.* 49 (1988) 2181;
H. Miyajima et al., *J. de Phys. Colloq.* 49 (1988) 2185.
- [11] R.L. Lichti et al., *Appl. Phys. Lett.* 54 (1989) 3261.